Cellulose (2021) 28:4211–4222
https://doi.org/10.1007/s10570-021-03811-z

ORIGINAL RESEARCH

Synthesis of plant oil derived polyols and their effects on the properties of prepared ethyl cellulose composite films

Yamei Lin · Mei Li · Jianling Xia · Haiyang Ding · Lina Xu · Xiaohua Yang · Shouhai Li

Received: 31 October 2020 / Accepted: 4 March 2021 / Published online: 19 March 2021

Abstract Polyols with different number of hydroxyl groups were synthesized from ricinoleic acid and oleic acid. These plant oil derived polyols can be used as plasticizers and combined with ethyl cellulose (EC) through supramolecular system to prepare ethyl cellulose composite films. The morphology, thermal stability and mechanical properties of the prepared ethyl cellulose films were studied in detail to indicate the plasticizing efficiency of these polyols and the effect of the number of hydroxyl groups in polyols on EC composite film's properties. With the addition of polyols, the tensile strength of EC composite films decreased, while the elongation at break increased. The elongation at break of EC composite films can be improved by 11–12 times when the polyols contain 1–3 hydroxyl groups. Thus, the plant oil derived polyols with 1–3 hydroxyl groups can be used as plasticizers for EC films. In addition, molecular dynamic simulations were performed to further probe the effects of the number of hydroxyl groups in polyols on EC composite film's properties.

Supplementary Information The online version contains supplementary material available at https://doi.org/10.1007/s10570-021-03811-z.

Y. Lin · M. Li (✉) · J. Xia · H. Ding · L. Xu · X. Yang · S. Li (✉)
Institute of Chemical Industry of Forestry Products, Jiangsu Province Biomass Energy and Materials Laboratory, Chinese Academy of Forestry, No. 16 Suojin 5th Village, Nanjing 210042, People's Republic of China
e-mail: meiyu20032001@126.com

S. Li
e-mail: lishouhai1979@163.com

Y. Lin
School of Food Science and Pharmaceutical Engineering, Nanjing Normal University, Nanjing 210023, People's Republic of China

Graphic abstract

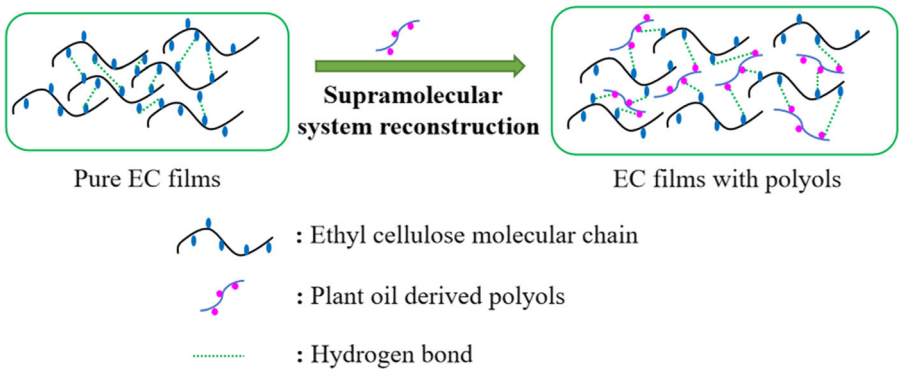

Keywords Plant oil · Polyols · Ethyl cellulose composite films · Supramolecular system · Flexibility

Introduction

Most membranes are derived from petro-chemical products, which will lead to the increased emission of carbon dioxide and global warming (Halden 2010; Etxabide et al. 2016). Meanwhile, these petroleum-based films cannot be degraded after discard, thereby causing serious environmental pollution (Chen et al. 2012; Qin et al. 2010). With the increasing shortage of petroleum resources and a series of shortcomings that caused by using petroleum-based films, researchers began to turn their attention to developing bio-based films. For the preparation of bio-based films, starch, chitosan and lignin are commonly used raw materials (Landaeta et al. 2018; Pelissari et al. 2009).

Ethyl cellulose (EC), a derivative from the most abundant biomass molecule-cellulose, has properties such as good plasticity, biocompatibility, heat resistance and light resistance (Lu and Yuan 2017; Heredia-Guerrero et al. 2018; Chen et al. 2016). It is worth mentioning that ethyl cellulose shows good film-forming performance and the prepared films can be used for biological separation and microcapsule materials (Adikane and Iyer 2013; Es-haghi et al. 2014; Wu et al. 2018; Pang et al. 2017). Nevertheless, the rigid inter chain hydrogen bonds in EC films result in high glass transition temperature and brittle films, which limit application of EC in some fields (Bodmeier 1994).

Therefore, plasticizers are added to improve the flexibility and processability of EC films (Verhoeven et al. 2008; Rahman et al. 2004). Commonly used plasticizers are long chain esters such as dibutyl sebacate, triethylacetylated monoglyceride, triacetin and diethyl pathalate (Bueno-Ferrer et al. 2010; Vieira et al. 2011). However, such plasticizers cannot significantly improve the flexibility of EC films (Hyppölä et al. 1996), and some of them have been strictly banned for use in medical and children products in some countries due to their toxic nature (Peña et al. 2000; Krauskopf 2003). For the sake of sustainable development, bio-based plasticizers have been investigated, such as triethyl citrate, vegetable oil-derived dimer acid and epoxidized soybean oil. These bio-based plasticizers can effectively improve the flexibility or reduce the glass transition temperature of EC films (Tarvainen et al. 2003; Lee et al. 2015; Yang et al. 2014).

However, most plasticizers mentioned above have large spatial structure and may leach out of the films during a long period of time. In our previous work, a ricinoleic acid-based sulfhydryl triol was synthesized and used as an efficient plasticizer for EC films through the construction of a stable supramolecular system (Li et al. 2017). There are two key points for the construction of excellent supramolecular system: (1) Moderate intermolecular force is required between plasticizers and EC molecules, because too strong interaction will lead to worse flexibility of EC composite film while too weak interaction will lead to an unstable supramolecular system. (2) The plasticizers preferably have long fatty chains and small spatial structure, which are helpful for them to insert between EC molecular chains. As we know, hydroxyl is a typical group that can take part in the formation of hydrogen bonds, and plant oils contain flexible fatty chains. From this perspective, the plant oil derived

polyols may have the potential to improve the properties of EC films by constructing a supramolecular system.

In this paper, we have synthesized a series of polyols with different number of hydroxyl groups from ricinoleic acid and oleic acid, which are the products of plant oils (Scheme 1). Although the preparation of these polyols requires multiple steps, the reactions involved in the preparation process are simple and well-developed with easy work-up procedure. This work can not only broaden the application fields of sustainable ethyl cellulose, but also promote the high-value use of cheap plant oil. These plant oil derived polyols have been applied in the preparation of EC composite films, and their effects on the properties of EC films were also studied by thermal gravity analysis, dynamic mechanical analysis, tensile test, scanning electron microscopy and dynamic simulation method.

Materials and methods

Raw materials

Ricinoleic acid (> 97 % (T), > 70 % (GC), oleic acid (AR), sodium hydroxide (97 %) and benzyl triethyl ammonium chloride (98 %) were purchased from Aladdin Industrial Corporation Co., Ltd., China. Mercaptoethanol (99 %) was purchased from Shandong Xiya Chemical Industry Co. Ltd., China. Allyl bromide (99 %) was purchased from Shanghai Adamas Reagent Co. Ltd., China. Calcium oxide was supplied by the Xilong Chemical Company, China. Hydrogen peroxide (30 %), acetic acid (≥ 99.5 %) and acetone (≥ 99.5 %) were purchased from Nanjing Chemical Reagent Co. Ltd., China. Formic acid (99 %) was purchased from Sann Chemical Technology Co., Ltd, China. The epichlorohydrin (≥ 99.0 %) was purchased from Shanghai Lingfeng Chemical Reagent Co., Ltd, China. Ethyl cellulose M70 (viscosity: 40.0–100.0 cPa s, the content of ethoxy group: 43–50%, the degree of polymerization:

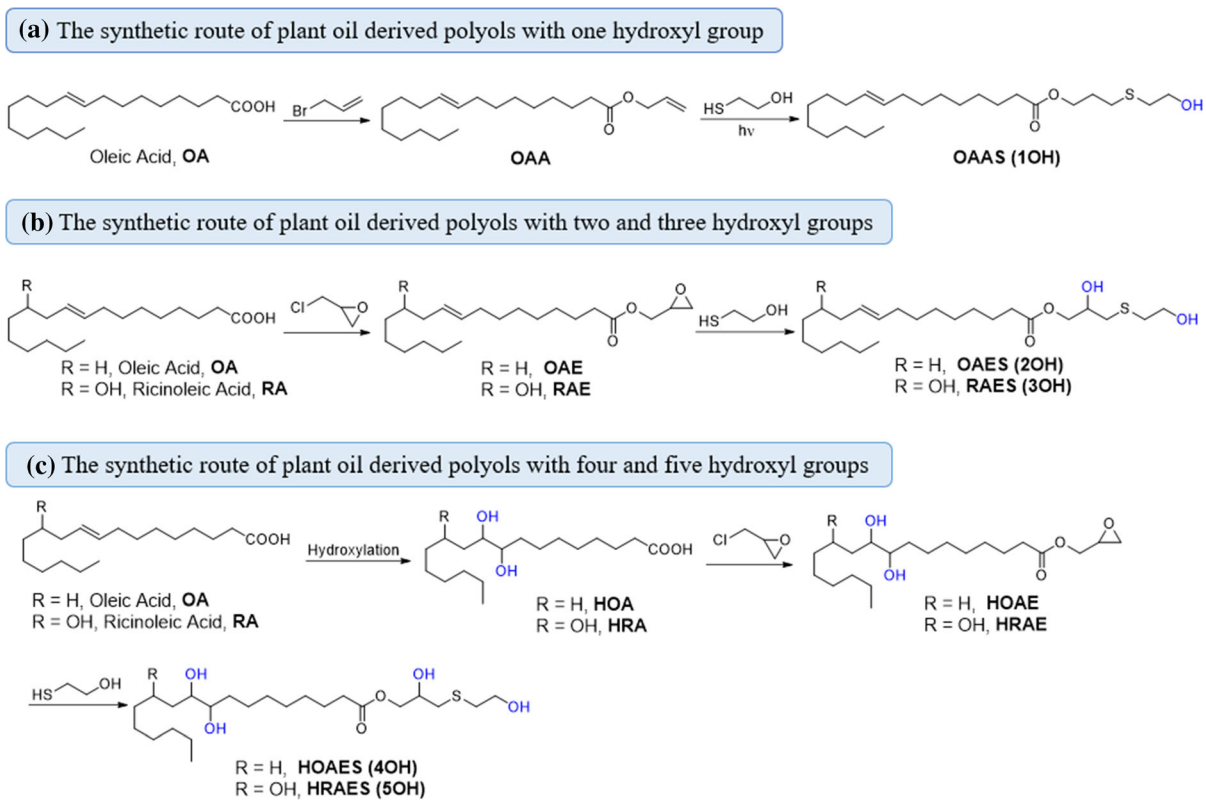

Scheme 1 The synthetic routes of plant oil derived polyols

365–376, the molecular weight of ethyl cellulose was determined by gel permeation chromatography, and the Mw is 74,489) was obtained from the Sinopharm Chemical Reagent Co., Ltd, China. All the chemicals were used as received without further purification.

Synthesis of plant oil derived polyols

The preparation routes of plant oil derived polyols are shown in Scheme 1. For the preparation of HOAES (4OH), firstly, the OA (30 g, 106 mmol), formic acid (9.5 g, 31.55% of the mass of OA) and *p*-toluene sulfonic acid (381 mg, 1.27 % of the mass of OA) were added into a 4-neck round-bottom flask and heated to 50 °C. Then, hydrogen peroxide (24.7 g, 82.45 % of the mass of OA) was slowly added with a dropping funnel. After that, the mixture was slowly heated to 65 °C and keep stirring for 5 h. Finally, 20 mL of ethyl acetate and 10 mL of water were added to the reaction mixture and stirred for 10 min. After the reaction was completed, the oil layer of reaction mixture was separated by a separatory funnel and washed with 30 mL water for three times. And then the oil layer was dried with anhydrous Na_2SO_4 and the residual solvent in oil layer was evaporated by vacuum distillation to obtain HOA (27.9 g, 83.4 % yield).

Secondly, the HOA (20 g, 63.3 mmol), epichlorohydrin (58.5 g, 633mmol) and benzyl triethyl ammonium chloride (144 mg, 0.633 mol) were added into a 4-neck round bottom flask and reacted at 100 °C for 3 h. After the reaction mixture was cooled to 60 °C, sodium hydroxide (3 g, 75 mmol) and calcium oxide (4.2 g, 75 mmol) were added and reacted at 60 °C for 6 h. Finally, the reaction mixture was filtered and the filtrate was collected. The excess epichlorohydrin was removed by vacuum distillation from the filtrate and the product HOAE was obtained (19.9 g, 84.5 % yield).

Thirdly, the HOAE (15 g, 40 mmol), mercaptoethanol (3.1 g, 40 mmol) and DMP-30 (450 mg, 3% of the mass of HOAE) were added into a 4-neck round bottom flask and reacted at 120 °C for 3 h to obtain the target product HOAES (4OH).

The preparation method of HRAES (5OH) is the same as that of HOAES (4OH), except that the starting material is changed from OA to RA. In addition, the preparation methods for OAAS (1OH), OAES (2OH) and RAES (3OH) are listed in the supplementary data (Scheme S1).

Preparation of ethyl cellulose composite films

EC films with or without the addition of plant oil derived polyols were prepared and labeled as pure EC, EC-OAAS (1OH), EC-OAES (2OH), EC-RAES (3OH), HOAES (4OH) and HRAES (5OH). In the preparation of EC composite films, the mass ratio of polyols and ethyl cellulose is 3:7. Take the preparation of EC-OAAS (1OH) as an example. 1.75 g of EC was dissolved in acetic acid at 80 °C for 2 h to make 7.3 % (w/w) solutions. Then 750 mg of OAAS (1OH) was mixed with 7.3 % EC solutions and stir at 80 °C for 5 min. Subsequently, the solution was transferred into clean polypropylene mold with casting area of 70 mm × 100 mm and dried at room temperature for 16 h. Finally, EC-OAAS (1OH) was obtained after further drying at 80 °C for 4.5 h. Preparation of pure EC films, EC-OAES (2OH), EC-RAES (3OH), EC-HOAES (4OH) and EC-HRAES (5OH) were consistent with above method. The residual amount of acetic acid in the films were measured and the mass fraction of acetic acid is 0.11 % ~ 0.36 %. The residual amount of acetic acid was calculated by the following formula:

$$\text{The mass fraction of acetic acid} = \frac{W_{film} - W_{EC} - W_{polyol}}{W_{film}}$$

W_{film} the weight of EC composite film, W_{EC} the weight of EC, W_{polyol} the weight of polyol.

Characterization

The chemical structures of films were confirmed by FTIR spectra (Nicolet IS10 instrument, USA) by an attenuated total reflectance method in a range of 4000–550 cm^{-1} wavenumbers with a resolution of four cm^{-1}.

Thermal gravimetric analysis (TGA) was performed using a NETZSCH STA 409 PC (Netzsch Instrument Crop., Germany). Each sample was put into platinum pans under nitrogen atmosphere at a rate of 20 mL/min and scanned from 40 to 800 °C at a rate of 15 °C/min.

Dynamic mechanical analysis (DMA) of the EC supramolecular composite films were performed using a dynamic mechanical analyzer (Rheometric Scientific IV). The sample size was approximately 18 mm (L) × 7 mm (W) × 0.4 mm (T). Samples were subjected to stretching mode at an oscillatory

frequency of 1 Hz. The testing temperature was swept from − 80 to 150 °C at a rate of 3 °C/min.

Tensile strength was measured by an E43.104 Universal Testing Machine (MTS Instrument Crop., China). The standard applied for tensile strength and elongation at break was GB/T 13022-91 (China). The specimens' size was approximately 50 mm (L) × 4 mm (W) × 0.2 mm (T). Five specimens were tested with a crosshead speed of 5mm/min under a fixed temperature of 23 °C and the average values were obtained.

The micrographs of the EC films' fracture surface were taken by scanning electron microscopy (SEM) (Hitachi S3400-N, Japan). The fracture surface of EC films was obtained by cryofracture with the help of liquid nitrogen. In order to avoid electrostatic charging during the examination, the exposed fracture surface was coated with gold. The methodology used to coat the EC films is plasma sputtering coating process and the thickness of the gold film obtained is around 10 nm.

The ^{1}H-NMR spectra were recorded on an AVANCE III HD 400 MHz spectrometer at ambient temperature. The $CDCl_3$ was used as the sample solvent and the concentration of sample was controlled at around 20 mg/mL.

Molecular dynamic simulation method

Molecular dynamics (MD) simulations were performed to investigate the mechanism. The condensed-phased-optimized molecular potential for atomistic simulation studies force field has been employed to optimized. In the modeling, the structure initially constructed with anions and cations in order to reach a better property. Our simulation structure are established. In addition, the complex is also applied hexagonal symmetry to construct our model, and the cell size is 23.63 × 23.62 × 23.62 Å. To obtain a global minimum energy configuration, a geometry optimization is first performed using the method of conjugate-gradient with a convergence criteria of 0.00001 kcal/mol. The unit cells are then allowed to equilibrate over NPT simulations (isothermal-isobaric ensemble) at a room temperature of 298 K and atmospheric pressure of 101 KPa for 20 ns with a time step of 1 fs. The requilibration molecular systems can be obtained after a geometry optimization. These simulation processes are aimed to remove internal stresses in the structure. In addition, a potential cut off radii of 2.25 nm is applied in the calculation of the nonbonded interaction. Andersen feedback thermostat and Berendsen barostat algorithm are applied in the system temperature and pressure conversion. The Ewald summation method with an accuracy of 0.001 kcal/mol is used in calculations of the electrostatic interactions. Finally, the properties have been calculated within last 80 ps and temperature.

Results and discussion

FTIR and ^{1}H NMR analysis of OA, HOA, HOAE and HOAES (4OH)

Figure 1 shows the FTIR spectra of OA, HOA, HOAE, mercaptoethanol and HOAES (4OH). In the FTIR spectrum of OA, the absorption at 1704 cm^{-1} and 3009 cm^{-1} correspond to the carboxyl group and double bond in OA, respectively. Compared to the FTIR spectrum of OA, it can be observed that the peak at 3009 cm^{-1} disappeared in the spectrum of HOA. In addition, there is a new peak at around 3388 cm^{-1} belonging to stretching vibration of hydroxyl group, indicating the double bond on OA was completely hydroxylated. Compared to the FTIR spectrum of HOA, the absorption peak at 1708 cm^{-1} disappear and the peaks of ether group at 1734 cm^{-1} and epoxy group at 910 cm^{-1} appear, indicating that the carboxyl group in HOA was react with epichlorohydrin to

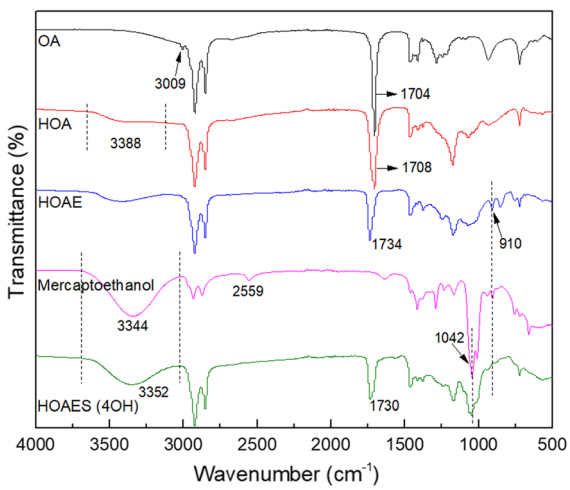

Fig. 1 FTIR spectra of OA, HOA, HOAE, mercaptoethanol and HOAES (4OH)

form HOAE. In the FTIR spectrum of mercaptoethanol, the peaks of 3344 cm^{-1} and 1042 cm^{-1} are attributed to stretching vibration and bending vibration of hydroxyl group, respectively, and the peaks at 2559 cm^{-1} is attributed to stretching vibration of S-H. Compared to the FTIR spectrum of HOAE, the disappearance of peaks at 910 $cm^{-1}$and the new peak at 1042 cm^{-1} can be explained by the successful nucleophilic substitution reaction of the epoxy group in HOAE and mercaptoethanol, forming the final product HOAES (4OH).

The ^{1}H NMR spectra of OA, HOA, HOAE and HOAES (4OH) are shown in Fig. 2 and the attributions of the chemical shifts of the protons are labeled in the figure. Compared to the ^{1}H NMR spectrum of OA, the peaks at around 5.5 ppm and 2.1 ppm shifted to 3.3–3.8 ppm and 1.5 ppm, respectively, indicating that the double bond in OA was completely hydroxylated and transformed to HOA. Compared to the ^{1}H NMR spectrum of HOA, there are new peaks at around 3.8–4.5 ppm (the peaks of protons on 19th carbon), 3.2 ppm (the peaks of protons on 20th carbon) and 2.75–3.0 ppm (the peaks of protons on 21th carbon) in the ^{1}H NMR spectrum of HOAE, indicating the presence of methylene epoxy group. Compared to the ^{1}H NMR spectrum of HOAE, the peaks of protons on 19th carbon, 20th carbon and 21th carbon in the spectrum of HOAES (4OH) shifted respectively, and new peaks appear at around 2.9 and 3.75 ppm, indicating that the mercaptoethanol successfully attacked the epoxy ring on HOAE to form HOAES (4OH).

The FTIR and ^{1}H NMR analysis of OAAS (1OH), OAES (2OH), RAES (3OH) and HRAES (5OH) as well as a series of corresponding intermediates are summarized in the Supplementary data (Fig. S1–S4).

FTIR analysis of pure EC and EC composite films

Figure 3 shows the FTIR spectra of EC, EC-OAAS (1OH), EC-OAES (2OH), EC-RAES (3OH), EC-HOAES (4OH) and EC-HRAES (5OH). In the spectrum of EC, the absorption peak at around 3476 cm^{-1} and 1055 cm^{-1} belong to the stretching vibration of O–H and C–O–C in ethyl cellulose, respectively. Compared to the spectrum of EC, it can be seen that new peak at around 1739 cm^{-1} appeared in EC-OAAS (1OH), EC-OAES (2OH), EC-RAES (3OH), EC-HOAES (4OH) and HRAES (5OH), belonging to the ester carbonyl group in polyols. In addition, as can be seen from the FTIR spectra of EC films with polyols (Fig. 3) and the curve fit analysis of peak width at

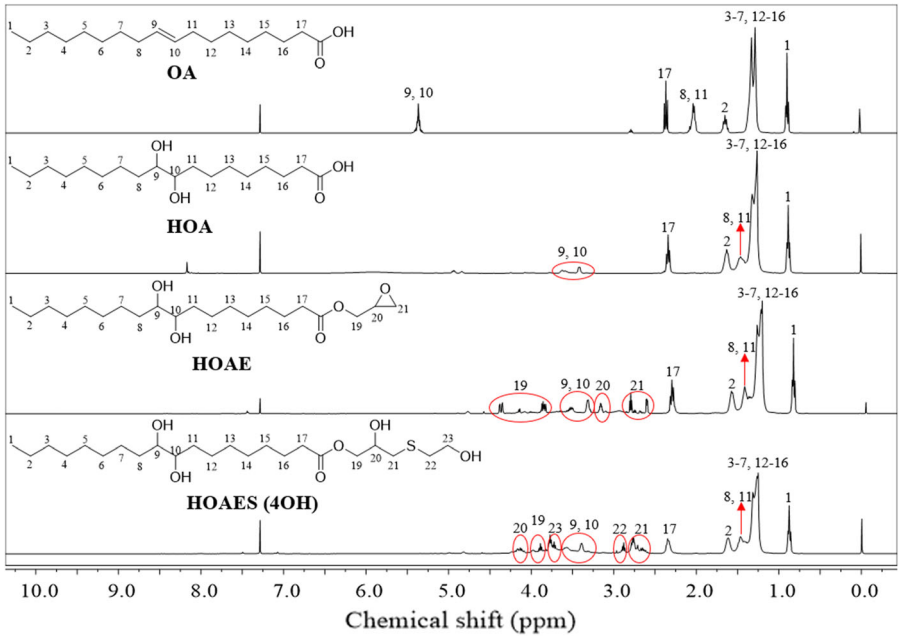

Fig. 2 ^{1}H NMR spectra of OA, HOA, HOAE and HOAES (4OH). $CDCl_3$ was used as the solvent of the samples and the NMR frequency is 400 MHz

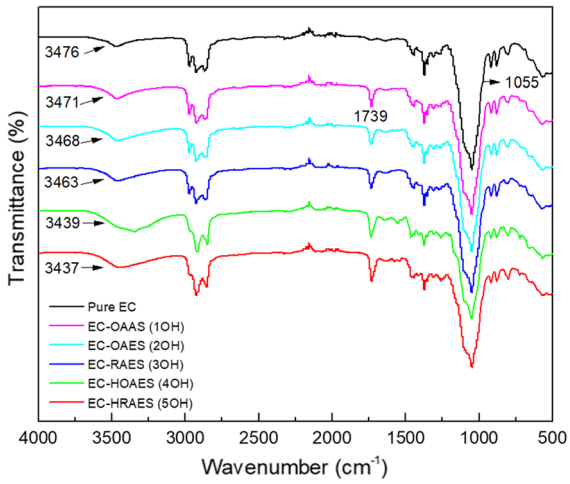

Fig. 3 FTIR spectra of pure EC and EC composite films

3476 cm^{-1} (Fig. S5), the peak belonging to the stretching vibration of O–H shifted to lower frequency and the width of which increased, due to formation of hydrogen bonds between polyols and ethyl cellulose and the force constant lowering in the bound state. Therefore, it can be observed that good supramolecular systems were formed by polyols and ethyl cellulose.

Morphology of pure EC and EC composite films

The electronic photos of the EC films with or without polyols are shown in the Supplementary data (Fig. S6). From the photos of EC, EC-OAAS (1OH), EC-OAES (2OH), EC-RAES (3OH), EC-HOAES (4OH) and EC-HRAES (5OH), it can be observed that the appearance of the films is relatively transparent, which imply the good compatibility of EC and polyols. Figure S6 (a_2–f_2) show the states of different EC films when bent by tweezer. The pure EC film is immediately broken into two pieces once bent by tweezer, whereas EC film with polyols stay intact. From this perspective, the addition of OAAS (1OH), OAES (2OH), RAES (3OH), HOAES (4OH) and HRAES (5OH) can improve the flexibility of obtained films to a certain extent.

Figure 4 shows the SEM images of EC films' exposed fractured surface. The large hindrance of EC molecule resulted in poor hydrogen bond system in pure EC film, causing many holes are visible in the fracture surface of pure EC film (a, a_1). From the photographs of b–d and b_1–d_1, it can be observed that the holes are decreased sharply in the fractured surface, indicating that OAAS (1OH), OAES (2OH) and RAES (3OH) can destroy the original hydrogen bond system in EC molecule and rebuild excellent supramolecular system with EC molecule. However, the fractured surface holes slightly increased when the number of hydroxyl groups in polyols reached to 4 and 5, implying that excessive hydroxyl groups are not conductive to the formation of supramolecular systems due to increased steric hindrance.

TGA analysis

The thermal stability of EC supramolecular composite films was evaluated by TGA and the relevant data was summarized in Table 1. The thermal data for EC films with 5 %, 10 % and 50 % mass loss temperature (T_5, T_{10} and T_{50}), and char yield at 450 °C and 600 °C (CY_{450} and CY_{600}) could be obtained from Table 1. It's obvious that EC films containing polyols are not as thermally stable as pure EC films, as the initial degradation temperature of pure EC film is 310.7 °C, while the EC films with polyols are 256.4–271.4 °C. In addition, compared with pure EC film, the T_{10}, T_{50}, CY_{450} and CY_{600} of most EC films containing polyols were lower. It can be explained that heat disrupts the hydrogen system between additives and EC molecules, leading to the overflow of polyols from films (Zhu et al. 2013). Furthermore, the TG analysis curves of pure EC and EC composite films were shown in Fig. S7, indicating that there is one stage of thermal decomposition in EC composition films.

Mechanical properties

The detailed mechanical data of different EC films were listed in Table 2 containing films' thickness, tensile strength, elongation at break and elasticity modulus. The elongation at break of pure EC film is only 1.80 %, indicating the brittle nature of pure EC film. With the addition of plant oil derived polyols, the elongation at break of EC composite films increased, while the tensile strength decreased. The elongation at break of EC composite films can be increased by 11–12 times than pure EC film when the polyols contain 1–3 hydroxyl groups. The main reason may be that the introduction of OAAS (1OH), OAES (2OH)

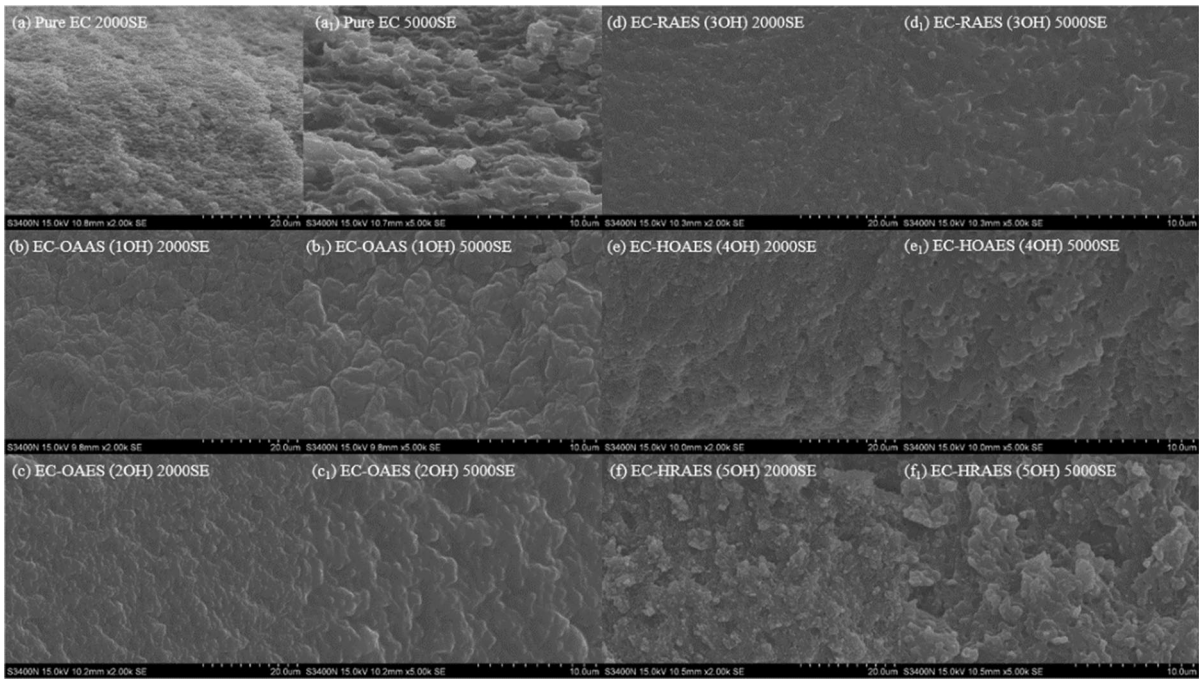

Fig. 4 SEM images of the fractured surface of EC films

Table 1 Detailed TGA analysis data of different EC films

Films	T_5[a] (°C)	T_{10}[a] (°C)	T_{50}[a] (°C)	CY_{450}[b] (%)	CY_{600}[b] (%)
Pure EC	310.7	330.7	363.2	7.3	5.4
EC-OAAS (1OH)	258.8	291.4	361.4	3.0	1.7
EC-OAES (2OH)	268.9	301.4	359.0	5.2	4.1
EC-RAES (3OH)	271.6	304.1	352.9	8.1	6.3
EC-HOAE (4OH)	261.5	301.4	352.7	6.1	4.4
EC-HRAES (5OH)	256.4	303.9	354.5	8.5	6.9

[a]T_5, T_{10} and T_{50} are the temperature at a weight loss of 5%, 10% and 50%, respectively

[b]CY_{450} and CY_{600} are the residue yield at 450 °C and 600 °C, respectively

Table 2 The detail data of the mechanical properties of pure EC and EC composite films

Films	Thickness (mm)	Tensile strength (MPa)	Elongation at break (%)	Elasticity modulus (MPa)
Pure EC	0.16	12.96 ± 4.05	1.80 ± 4.05	251.71 ± 73.13
EC-OAAS (1OH)	0.23	5.90 ± 0.20	21.84 ± 2.07	220.44 ± 7.69
EC-OAES (2OH)	0.22	7.80 ± 0.57	19.27 ± 0.56	374.52 ± 15.71
EC-RAES (3OH)	0.23	8.17 ± 0.57	19.90 ± 0.61	351.02 ± 12.22
EC-HOAES (4OH)	0.22	11.47 ± 1.03	11.62 ± 0.98	585.43 ± 63.99
EC-HRAES (5OH)	0.20	13.73 ± 1.77	6.35 ± 1.15	755.13 ± 93.07

and RAES (3OH) can not only destroy the poor hydrogen bond system between EC molecular chains, but also bring in a long fat chain. Thereby, excellent supramolecular systems were established in EC-OAAS (1OH), EC-OAES (2OH) and EC-RAES (3OH), and the flexibility of EC composite films are improved. However, the elongation at break of EC films were sharply decreased when the number of hydroxyl groups in polyols reach to 4 and 5. This is because excessive hydroxyl groups leads to too tight interaction between polyols and EC molecules, which increases the rigidity of EC films and results in poor flexibility

DMA analysis

The dynamic mechanical properties of the EC films with different polyols were measured by DMA. Figure 5 shows the storage modulus (E′) and loss tangent (tanδ) of EC composite films as a function of temperature. From the change curve of lgE′ with temperature, it can be obtained that all curves have a similar decreasing trend. In addition, the storage modulus of EC films is not much affected by the polyols at low temperature (< − 40 °C), because the storage modulus is mainly determined by the chemical structure of polymers at low temperature. At high temperature (> 40°C), the storage modulus of EC films decreases with the addition of polyols, and varies with the number of hydroxyl groups in the polyols. This is because the storage modulus of EC films is mainly affected by hydrogen bond between macromolecules at high temperature region (Cao et al. 2018). The insertion of polyols will destroy the rigid inter chain hydrogen bond system of EC to rebuild a new supramolecular system, and introduce a flexible fat chain with plasticizing effect at the same time. The storage modulus is relatively low when the additives contain 1–3 hydroxyl groups, whereas the storage modulus become higher when the number of hydroxyl groups reaches 4–5. This can be interpreted that more hydroxyl groups will lead to stronger intermolecular interaction, resulting in more rigid polymers.

According to the change curve of tan δ with temperature, the glass transition temperature (T_g) of EC films can be obtained. A single tan δ is observed at per peak, indicating that the EC composite films are homogeneous. The T_g of pure EC film is 154.0 °C, which is similar with the temperature reported in previous work (Lee et al. 2015; Lai et al. 2010). With the addition of polyols with 1–5 hydroxyl groups, the T_g of EC composite films decreases and exhibits T_g at a temperature range of 64.9–120.9 °C. In the report of Lee et al. (Lee et al. 2015), the EC film containing 30 % DOP (dioctyl phthalate) exhibits T_g at a temperature range of 30–80 °C, which has similar effect as the addition of 30 % polyols with 1–3 hydroxyl groups. Therefore, OAAS (1OH), OAES (2OH) and RAES (3OH) can be effective plasticizers for EC films.

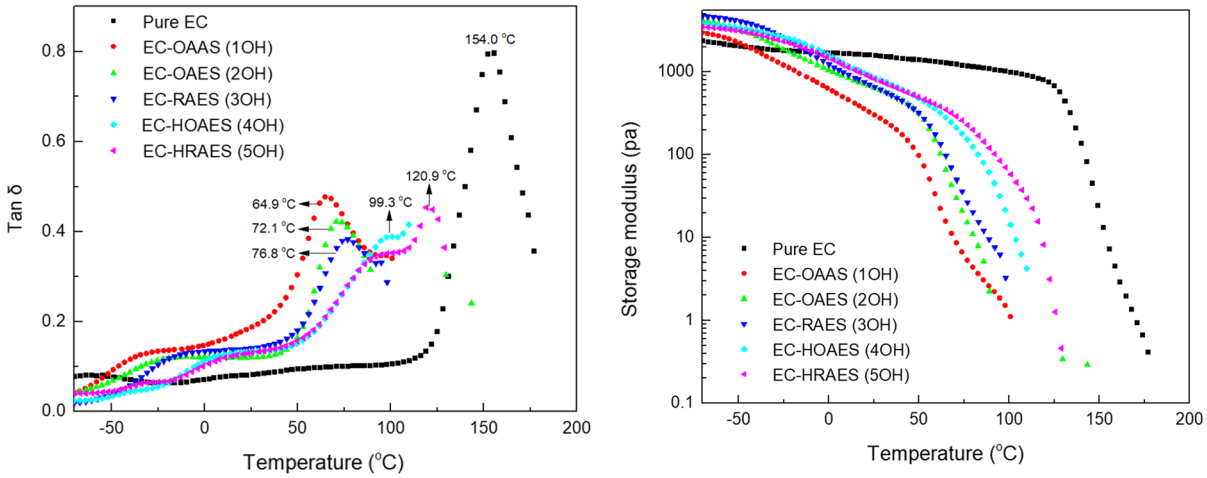

Fig. 5 Storage modulus (E′) and loss factor (tanδ) of different EC films

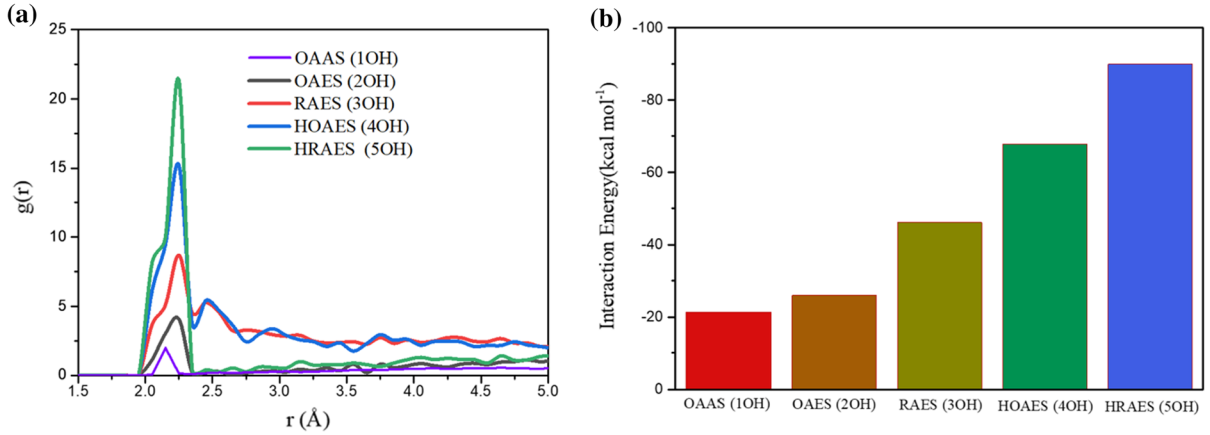

Fig. 6 Molecular dynamic simulation results. **a** The radius distribution function (rdf) plot versus the center of mass (COM) distance *r* between the polyols and ethyl cellulose; **b** the interaction energy of different polyols with ethyl cellulose as a function of different polyols

Molecular dynamic simulation results

In the radius distribution function (rdf) plot in panel (a) as a function of the center of mass distance (COM) between the polyols and ethyl cellulose, from locating the x-coordinate of the rdf peak, we found the OAAS (1OH) bears the largest binding distance from the ethyl cellulose in the bound state, and the binding distance decreased as the number of polyols' hydroxyl groups increased. In accordance with the results of Fig. 6a, it can be observed from Fig. 6b that the interaction energy of polyols with ethyl cellulose decreased as the number of polyols' hydroxyl groups increased. Thus, the molecular dynamic simulation results can be applied to support the previous statement in this paper that more hydroxyl groups in polyols leaded to stronger intermolecular interaction between polyols and ethyl cellulose.

Conclusions

In summary, plant oil derived polyols were used as the plasticizers for EC films through the construction of supramolecular systems. The EC composite films containing polyols are not as thermally stable as pure EC films, as the initial degradation temperature of pure EC film is 310.7 °C, while the EC composite films with polyols are 256.4–271.4 °C. However, the introduction of polyols can efficiently improve the flexibility of prepared EC composite films. With the addition of plant oil derived polyols, the tensile strength of EC composite films decreases, while the elongation at break increases. The polyols with 1–3 hydroxyl groups show excellent plasticizing effect, as the elongation at break of EC composite films can be increased by 11–12 times. However, when the hydroxyl group of the polyols increase to 4 or 5, their plasticizing ability is greatly reduced. In addition, the introduction of polyols also reduce the glass transition temperature of EC composite films. The T_g of pure EC is 154.0 °C, and the T_g of EC composite films containing different number of hydroxyl groups are varied from 64.9 °C to 120.9 °C. Therefore, the plant oil derived polyols with 1–3 hydroxyl groups can be used to plasticize EC films, so that to obtain bio-based films with good flexibility. In addition, the results of molecular dynamic simulations further verified that more hydroxyl groups in polyols leaded to stronger intermolecular interaction between polyols and ethyl cellulose.

Acknowledgments This work was supported by Major projects of National Natural Science Foundation of China (Grant No. 31890773), Jiangsu Province Biomass Energy and Materials Laboratory, China (Grant No. JSBEM-S-202007) and the National Natural Science Foundation of China (Grant No. 32001266).

References

Adikane HV, Iyer GJ (2013) Chemical modification of ethyl cellulose-based highly porous membrane for the purification of immunoglobulin G. Appl Biochem Biotechnol

169:1026–1038. https://doi.org/10.1007/s12010-012-0085-y

Bodmeier R, Paeratakul O (1994) Mechanical properties of dry and wet cellulosic and acrylic films prepared from aqueous colloidal polymer dispersions used in the coating of solid dosage forms. Pharmaceut Res 11:882–888. https://doi.org/10.1023/A:1018942127524

Bueno-Ferrer C, Garrigós M, Jimenez A (2010) Characterization and thermal stability of poly(vinyl chloride) plasticized with epoxidized soybean oil for food packaging. Polym Degrad Stabil 95:2207–2212. https://doi.org/10.1016/j.polymdegradstab.2010.01.027

Cao S, Li S, Li M, Xu L, Ding H, Xia J, Zhang M, Huang K (2018) The thermal self-healing properties of phenolic polyurethane derived from polyphenols with different substituent groups. J Appl Polym Sci 136:47039. https://doi.org/10.1002/app.47039

Chen GQ, Patel MK (2012) Plastics derived from biological sources: present and future: a technical and environmental review. Chem Rev 112:2082–2099. https://doi.org/10.1021/cr200162d

Chen J, Wu D, Pan K (2016) Effects of ethyl cellulose on the crystallization and mechanical properties of poly(β-hydroxybutyrate). Int J Biol Macromol 88:120–129. https://doi.org/10.1016/j.ijbiomac.2016.03.048

Es-haghi H, Mirabedini SM, Imani M, Farnood RR (2014) Preparation and characterization of pre-silane modified ethyl cellulose-based microcapsules containing linseed oil. Colloids Surfaces A 447:71–80. https://doi.org/10.1016/j.colsurfa.2014.01.021

Etxabide A, Leceta I, Cabezudo S, Guerrero P, de la Caba K (2016) Sustainable fish Gelatin films: from food processing waste to compost. ACS Sustain Chem Eng 4:4626–4634. https://doi.org/10.1021/acssuschemeng.6b00750

Halden RU (2010) Plastics and health risks. Annu Rev Public Health 31:179–194. https://doi.org/10.1146/annurev.publheatth.012809.103714

Heredia-Guerrero JA, Ceseracciu L, Guzman-Puyol S, Paul UC, Alfaro-Pulido A, Grande C, Vezzulli L, Bandiera T, Bertorelli R, Russo D, Athanassiou A, Bayer IS (2018) Antimicrobial, antioxidant, and waterproof RTV silicone-ethyl cellulose composites containing clove essential oil. Carbohydr Polym 192:150–158. https://doi.org/10.1016/j.carbpol.2018.03.050

Hyppölä R, Husson I, Sundholm F (1996) Evaluation of physical properties of plasticized ethyl cellulose films cast from ethanol solution Part I. Int J Pharmaceut 133:161–170. https://doi.org/10.1016/0378-5173(96)04436-5

Krauskopf L (2003) How about alternatives to phthalate plasticizers? J Vinyl Addit Technol 9:159–171. https://doi.org/10.1002/vnl.10079

Lai HL, Pitt K, Craig DQM (2010) Characterisation of the thermal properties of ethylcellulose using differential scanning and quasi-isothermal calorimetric approaches. Int J Pharmaceut 386:178–184. https://doi.org/10.1016/j.ijpharm.2009.11.013

Landaeta E, Schultz ZD, Burgos A, Schrebler R, Isaacs M (2018) Enhanced photostability of cuprous oxide by lignin films on glassy carbon electrodes in the transformation of carbon dioxide. Green Chem 20:2356–2364. https://doi.org/10.1039/c8gc00365c

Lee S, Ko KH, Shin J, Kim NK, Kim YW, Kim JS (2015) Effects of the addition of dimer acid alkyl esters on the properties of ethyl cellulose. Carbohydr polym 121:284–294. https://doi.org/10.1016/j.carbpol.2014.12.029

Li M, Xia J, Ding C, Mao W, Ding H, Xu L, Li S (2017) Development and characterization of ricinoleic acid-based sulfhydryl thiol and ethyl cellulose blended membranes. Carbohydr Polym 175:131–140. https://doi.org/10.1016/j.carbpol.2017.07.069

Lu Y, Yuan W (2017) Superhydrophobic/superoleophilic and reinforced ethyl cellulose sponges for oil/water separation: synergistic strategies of cross-linking, carbon nanotube composite, and nanosilica modification. ACS Appl Mater Interfaces 9:29167–29176. https://doi.org/10.1021/acsami.7b09160

Pang L, Gao Z, Feng H, Wang S, Ma R, Zhou B, Hu S, Jin K (2017) Synthesis of a fluorescent ethyl cellulose membrane with application in monitoring 1-naphthylacetic acid from controlled release formula. Carbohydr polym 176:160–166. https://doi.org/10.1016/j.carbpol.2017.07.057

Pelissari FM, Grossmann MVE, Yamashita F, Pineda EAG (2009) Antimicrobial, mechanical, and barrier properties of cassava starch-chitosan films incorporated with oregano essential oil. J Agr Food Chem 57:7499–7504. https://doi.org/10.1021/jf9002363

Peña J, Hidalgo M, Mijangos C (2000) Plastification of poly(-vinyl chloride) by polymer blending. J Appl Polym Sci 75:1303–1312. https://doi.org/10.1002/(SICI)1097-4628(20000307)75:10<1303::AID-APP12>3.0.CO;2-4

Qin Y, Wang X (2010) Carbon dioxide-based copolymers: environmental benefits of PPC, an industrially viable catalyst. Biotechnol J 5:1164–1180. https://doi.org/10.1002/biot.201000134

Rahman M, Brazel CS (2004) The plasticizer market: an assessment of traditional plasticizers and research trends to meet new challenges. Prog Polym Sci 29:1223–1248. https://doi.org/10.1016/j.progpolymsci.2004.10.001

Tarvainen M, Sutinen R, Peltonen S, Mikkonen H, Maunus J, Vähä-Heikkilä K, Lehto VP, Paronen P (2003) Enhanced film-forming properties for ethyl cellulose and starch acetate using n-alkenyl succinic anhydrides as novel plasticizers. Eur J Pharm Sci 19:363–371. https://doi.org/10.1016/S0928-0987(03)00137-4

Verhoeven E, De Beer TRM, Van den Mooter G, Remon JP, Vervaet C (2008) Influence of formulation and process parameters on the release characteristics of ethylcellulose sustained-release mini-matrices produced by hot-melt extrusion. Eur J Pharm Biopharm 69:312–319. https://doi.org/10.1016/j.ejpb.2007.10.007

Vieira M, Silva M, Santos L, Beppu M (2010) Natural-based plasticizers and biopolymer films: a review. Eur Polym J 47:254–263. https://doi.org/10.1016/j.eurpolymj.2010.12.011

Wu K, Zhu Q, Qian H, Xiao M, Corke H, Nishinari K, Jiang F (2018) Controllable hydrophilicity–hydrophobicity and related properties of konjac glucomannan and ethyl cellulose composite films. Food Hydrocolloid 79:301–309. https://doi.org/10.1016/j.foodhyd.2017.12.034

Yang D, Peng X, Zhong L, Cao X, Chen W, Zhang X, Liu S, Sun R (2014) "Green" films from renewable resources:

properties of epoxidized soybean oil plasticized ethyl cellulose films. Carbohydr Polym 103:198–206. https://doi.org/10.1016/j.carbpol.2013.12.043

Zhu J, Shen W, Gao L, Gu H, Shen S, Wang Y, Wu H, Guo J (2013) PI3K/Akt-independent negative regulation of JNK signaling by MKP-7 after cerebral ischemia in rat hippocampus. BMC Neurosci 14:1. https://doi.org/10.1186/1471-2202-14-1